



HAL
open science

Potential and limitations of on-line comprehensive reversed phase liquid chromatographyxsupercritical fluid chromatography for the separation of neutral compounds: An approach to separate an aqueous extract of bio-oil

Morgan Sarrut, Amélie Corgier, Gérard Crétier, Agnès Le Masle, Stéphane Dubant, Sabine Heinisch

► **To cite this version:**

Morgan Sarrut, Amélie Corgier, Gérard Crétier, Agnès Le Masle, Stéphane Dubant, et al.. Potential and limitations of on-line comprehensive reversed phase liquid chromatographyxsupercritical fluid chromatography for the separation of neutral compounds: An approach to separate an aqueous extract of bio-oil. *Journal of Chromatography A*, 2015, 1402, pp.124-133. 10.1016/j.chroma.2015.05.005 . hal-01176925

HAL Id: hal-01176925

<https://hal.science/hal-01176925>

Submitted on 30 Sep 2015

HAL is a multi-disciplinary open access archive for the deposit and dissemination of scientific research documents, whether they are published or not. The documents may come from teaching and research institutions in France or abroad, or from public or private research centers.

L'archive ouverte pluridisciplinaire **HAL**, est destinée au dépôt et à la diffusion de documents scientifiques de niveau recherche, publiés ou non, émanant des établissements d'enseignement et de recherche français ou étrangers, des laboratoires publics ou privés.

1 **Potential and Limitations of On-line Comprehensive Reversed Phase Liquid**
2 **Chromatography x Supercritical Fluid Chromatography for the Separation of**
3 **Neutral Compounds: An approach to Separate Aqueous Extract of Bio-oil.**

4
5 Morgan Sarrut¹, Amélie Corgier¹, Gérard Crétier¹, Agnès Le Masle², Stéphane
6 Dubant³, Sabine Heinisch^{1*}

7
8 ¹ *Université de Lyon, Institut des Sciences Analytiques, UMR CNRS UCBL ENS 5280, 5 rue de la*
9 *Doua, 69100 Villeurbanne, France*

10 ² *IFP Energies nouvelles, Rond-Point de l'échangeur de Solaize, BP3, 69360 Solaize, France*

11 ³ *Waters SAS, BP608, 78056 St Quentin en Yvelines, France*

12 * Corresponding author - Tel : +33(0)437 423 551 ; E-mail address : sabine.heinisch@univ-lyon1.fr

13
14 **Abstract**

15
16 On-line comprehensive Reversed Phase Liquid Chromatography x Supercritical Fluid
17 Chromatography (RPLC x SFC) was investigated for the separation of complex
18 samples of neutral compounds. The presented approach aimed at overcoming the
19 constraints involved by such a coupling. The search for suitable conditions (stationary
20 phases, injection solvent, injection volume, design of interface) are discussed with a
21 view of ensuring a good transfer of the compounds between both dimensions, thereby
22 allowing high effective peak capacity in the second dimension. Instrumental aspects
23 that are of prime importance in on-line 2D separations, were also tackled (dwell
24 volume, extra column volume and detection). After extensive preliminary studies, an
25 on-line RPLCxSFC separation of a bio-oil aqueous extract was carried out and
26 compared to an on-line RPLCxRPLC separation of the same sample in terms of
27 orthogonality, peak capacity and sensitivity. Both separations were achieved in 100
28 min. For this sample and in these optimized conditions, it is shown that RPLCxSFC
29 can generate a slight higher peak capacity than RPLCxRPLC (620 vs 560). Such a
30 result is essentially due to the high degree of orthogonality between RPLC and SFC

31 which may compensate for lesser peak efficiency with SFC as second dimension.
32 Finally, in the light of the current limitations of SFC instrumentation for on-line 2D
33 analyses, RPLCxSFC appears to be a promising alternative to RPLCxRPLC for the
34 separation of complex samples of neutral compounds.

35

36

37

38 **Keywords**

39 Supercritical fluid chromatography (SFC); RPLC x SFC; Comprehensive two-
40 dimensional chromatography; Biomass by-products

41 **1 Introduction**

42

43 Over the last decades, on-line comprehensive two-dimensional liquid chromatography
44 (LCxLC) has grown significantly in many application fields [1–4]. Liquid
45 chromatography provides a wide variety of separation modes including Reversed
46 Phase Liquid Chromatography (RPLC), Normal Phase Liquid Chromatography
47 (NPLC), Steric Exclusion Chromatography (SEC), Ion Exchange Chromatography
48 (IEC) and Hydrophilic Interaction Liquid Chromatography (HILIC). On-line coupling two
49 of these different techniques *via* an appropriate interface may produce a separation
50 system capable of generating a very high effective peak capacity in a reasonable
51 analysis time while avoiding sample loss and/or sample contamination [5].

52 To maximize the potential of a two-dimensional system, one of the key problems is to
53 find orthogonal conditions between the two dimensions in order to obtain a separation
54 that uses the largest possible fraction (γ) of the separation space [6]. In this regard,
55 NPLCxRPLC was shown to be very attractive for the separation of pharmaceutical
56 compounds [7]. However, in spite of a lower degree of orthogonality, RPLCxRPLC has
57 often been preferred to avoid peak deterioration associated with the incompatibility of
58 the mobile phase of first dimension with that of second dimension (stronger eluting
59 power or immiscibility) [2,8,9] and finally to obtain an interesting sample peak capacity
60 for the overall comprehensive system.

61 Bio-oil samples are mainly composed of small neutral compounds. Two very recent
62 papers [10,11] presented successful separation of aqueous bio-oil extracts by on-line
63 RPLCxRPLC with a retention space coverage close to 50% only. NPLCxRPLC could
64 be a possible solution to increase the utilized portion of the available space. In this
65 work, we experiment another option which consists in coupling RPLC to supercritical
66 fluid chromatography (RPLCxSFC). This approach was expected to be attractive
67 because of the variety of mechanisms that govern retention in these two
68 chromatographic systems [12]. West and Lesellier showed that polar stationary phases
69 in SFC tend to behave as in NPLC [13]. Little polar stationary phases were also found
70 to be attractive with SFC mobile phases as recently reported in a study which
71 compared their use in SFC and RPLC [14]. On-line SFCxRPLC was investigated by
72 François et al. [15] for the separation of fatty acids in fish oils and compared to on-line
73 RPLCxRPLC for the separation of the same sample. 92 % of the separation space was
74 occupied in SFCxRPLC versus 55 % in RPLCxRPLC. However, SFCxRPLC
75 arrangement needed a particular interface composed of two two-position/ten-port
76 switching valves equipped with two loops packed with octadecyl silica allowing both
77 the depressurization of the supercritical fluid and the trapping and focusing of the
78 analytes after an addition of water to the first dimension eluent and before the transfer
79 to the second dimension. The potential of RPLCxSFC was highlighted by Stevenson
80 et al. [16] in off-line mode. On-line RPLCxSFC has never been investigated yet. Here
81 we describe our development of on-line RPLCxSFC for the separation of aromatic
82 neutral compounds and an aqueous extract of bio-oil. With a liquid eluent in the first
83 dimension, the interface between the two dimensions is simpler than that used in
84 SFCxRPLC and similar to that used in RPLCxRPLC. Moreover, in the second
85 dimension, the low viscosity of SFC mobile phase allows very fast analysis, which is of
86 prime importance to increase peak capacity in on-line two-dimensional separations.
87 This paper deals with the choice of SFC stationary phase, the study of phenomena
88 resulting from the injection of a polar sample solvent into a supercritical mobile phase
89 and the experimental and instrumental aspects related to the interface. Finally, a
90 comparison between RPLCxSFC and RPLCxRPLC separations of the same aqueous
91 bio-oil extract is proposed in terms of orthogonality, effective peak capacity and
92 sensitivity.

94 **2 Experimental**

95 *2.1 Material and reagents*

96

97 Acetonitrile (ACN) (HPLC grade), methanol (MeOH) and acetone were purchased of
98 HPLC grade from Sigma-Aldrich (Steinheim, Germany). Water was obtained from an
99 Elga water purification system (Veolia water STI, Le Plessis Robinson, France).
100 Pressurized liquid CO₂ 3.0 grade (99.9%) was obtained from Air Liquide (Pierre Bénite,
101 France).

102 The synthetic sample for RPLCxSFC experiments was chosen among different
103 compounds known to be representative of those found in bio-oil aqueous samples [10].
104 It contains α -hydroxycumene, phenol, 2,4,6-trimethylphenol, 1-indanone, syringol,
105 angelica lactone, m-cresol, o-cresol, anisole, guaiacol, 5-methylfurfural and
106 phenylethanol. They were dissolved in water/ACN 85/15 v/v at the concentration of 50
107 mg/L. Physical properties of these twelve compounds are reported in Table 1. The
108 compounds were either obtained from Sigma-Aldrich or graciously given by IFP
109 Energies nouvelles (Solaize, France). The bio-oil aqueous sample was provided by
110 IFP Energies nouvelles.

111

112 *2.2 Columns*

113

114 Four columns (50x2.1 mm, 1.7 μ m) from Waters (Milford, MA, USA) were used under
115 SFC conditions : Acquity UPC² BEH-2EP, Acquity UPC² BEH, Acquity UPC² CSH
116 Fluoro-Phenyl and Acquity UPC² HSS C18. Three columns were used under RPLC
117 conditions : XBridge C18 (50x1.0 mm 3.5 μ m) from Waters, Hypercarb (100x1 mm, 5
118 μ m) from Thermo Scientific (Cheshire, UK) and Acquity CSH Phenyl-Hexyl (50x2.1
119 mm, 1.7 μ m) from Waters.

120

121 *2.3 Apparatus*

122

123 1D-SFC system

124 Waters Acquity UPC² system was equipped with a binary solvent delivery pump, a 250
125 μL mixing chamber, an autosampler with a 10 μL loop, two column ovens compatible
126 with temperature up to 90°C and including two 6-channel column selection valves, a
127 UV detector with a 8 μL flow-cell and a backpressure regulator (BPR). The allowed
128 maximum flow rate is 4 mL/min. The allowed maximum pressure is 410 bar for flow-
129 rates up to 3.25 mL/min. This limit pressure linearly decreases to 290 bar when the
130 flow rate increases to 4 mL/min. Data acquisition was performed by Empower software
131 (Waters). The extra-column volume and extra-column variance were measured under
132 liquid chromatographic conditions. They were equal to 83 μL and 132 μL^2 respectively.
133 The system dwell volume was estimated at 300 μL (see section 2.4.1.).
134

135 RPLCxRPLC system

136 The RPLCxRPLC system was a 2D-IClass liquid chromatograph from Waters. This
137 instrument includes two high-pressure binary solvent delivery pumps, an autosampler
138 with a flow-through needle of 15 μL , a column manager composed of two column ovens
139 with an allowed maximum temperature of 90°C and two 6-port high pressure two-
140 position valves acting as interface between the two separation dimensions, a UV
141 detector and a diode array detector equipped with 500 nL flow-cells. For the first
142 dimension, the allowed maximum pressure is 1280 bar for flow-rates up to 1 mL/min ;
143 it linearly decreases to 850 bar when flow rate increases to 2 mL/min. For the second
144 dimension, the maximum pressure is 1280 bar for flow-rates up to 1.4 mL/min ; this
145 limit linearly decreases to 1170 bar when flow rate increases to 2 mL/min. The
146 measured dwell volume was 110 μL and 120 μL for the first and second dimensions
147 respectively. A total extra-column volume of 12 μL and 17 μL and an extra-column
148 variance of 4 μL^2 and 9 μL^2 were determined for the first and the second dimension
149 respectively.

150 To ensure a fair comparison between RPLCxRPLC and RPLCxSFC experiments, the
151 original interface made of two 6-port valves was replaced by a 10-port high pressure
152 2-position valve (Vici Valco Instruments, Houston, USA) equipped with two identical
153 loops of 20 μL . Data acquisition, the instrumental control of the two dimensions and
154 the programming of the 10-port high pressure 2-position valve interface were
155 performed by Masslynx software (Waters).

156

157 RPLCxSFC setup

158 The first dimension consisted in the high-pressure binary solvent delivery pump, the
159 column manager and the diode array detector of the 2D-IClass apparatus. The second
160 dimension consisted in the high-pressure binary solvent delivery pump, the UV
161 detector and the BPR of the Acquity UPC² apparatus, set at 140 bar.

162 As in RPLCxRPLC, the 10-port high pressure 2-position valve was used as interface
163 between the two dimensions. It was equipped with two identical loops of 3 or 5 μL . A
164 30 cmx175 μm i.d. tubing was used between the mixer of SFC pump and the 10-port
165 2-position valve. A 56 cmx175 μm i.d. tubing was connected between the valve and
166 the 31.8 cmx175 μm i.d. preheater of the second dimension column. Finally, the UV
167 detector was connected to the column outlet by 30 cm x 175 μm i.d. tubing.
168 Instrumental characteristics were determined for the SFC second dimension : 300 μL
169 for the dwell volume, , 57 μl for the extra-column volume and 50 μL^2 for the extra-column
170 variance. The RPLCxSFC setup is presented in Figure 1.

171 Both instrument control for the first dimension and interface programming were
172 performed by Masslynx software. Data acquisition and instrument control for the
173 second dimension were performed by Empower software dedicated to Acquity UPC²
174 instrument. Synchronization between both dimensions was obtained by connecting
175 electrically the two systems and by using external events in the first dimension method
176 controlled by Masslynx software.

177

178 2.4 Chromatographic procedures

179

180 1D-SFC

181 In LC the dwell volume, V_D , is usually determined from a gradient experiment
182 performed without column using MeOH as solvent A and MeOH + 0.1% acetone as
183 solvent B. The gradient is programmed on a wide range of composition, typically from
184 1 to 99% B, in order to minimize the uncertainty on V_D value. This latter is obtained by
185 multiplying the measured dwell time, t_D , by the flow rate used to perform the gradient
186 experiment. t_D is calculated from the time, t^* , corresponding to the half-part of the UV
187 signal between the start and the end of the gradient ($t_D = t^* - t_G / 2$, t_G being the
188 gradient time). For V_D determination, SFC mobile phases are composed with CO_2 as
189 solvent A and MeOH + 0.1% acetone as solvent B. It was found that when the initial
190 composition of the programmed gradient was rich in CO_2 (e.g. 1 %B), the obtained

191 gradient profile was not perfectly linear, which led to a high uncertainty Δt on the
192 gradient middle time t^* and consequently on the dwell volume V_D (Fig. 2a). From the
193 experiment shown in Fig.2a, V_D was in fact estimated at $600 \pm 300 \mu\text{L}$. This abnormal
194 behavior is likely to be due to the supercritical nature of the mobile phase at high
195 percentages of CO_2 . In order to correctly assess V_D in SFC, the gradient was therefore
196 started with a higher percentage of MeOH + 0.1% acetone (i.e. 69% B) in order to get
197 a quasi-liquid phase since the beginning of the gradient. Under these conditions the
198 observed gradient profile was actually linear as shown in Fig. 2 b and thus, the dwell
199 volume measurement was much more reliable (i.e. $300 \pm 40 \mu\text{L}$).

200 The compatibility of the four SFC stationary phases (Acquity UPC² HSS C18, Acquity
201 UPC² CSH FP, Acquity UPC² BEH and Acquity UPC² BEH-2EP) with LC injection
202 solvents composed of different water/ACN proportions was tested in isocratic
203 conditions, namely 95/2.5/2.5 $\text{CO}_2/\text{MeOH}/\text{CAN}$. The temperature, the flow rate, the
204 BPR, the wavelength and the sampling rate were set at 45 °C, 2.7 mL/min, 140 bar,
205 215 nm (compensation from 350 to 450 nm) and 40 Hz respectively for all the
206 experiments. The effect of injection solvent composition on the peak shape of o-cresol
207 was only studied with the Acquity UPC² BEH-2EP column. The flow rate was set at 2.2
208 mL/min. Other conditions were those mentioned above.

209 RPLCxSFC

210 RPLCxSFC experiments related to the effect of RPLC solvent injection on pressure
211 increase in second dimension were performed with the following conditions. In first
212 dimension, X-Bridge BEH C18 column was used with mobile phase consisted in Water
213 (A) and ACN (B); the gradient profile was : 0 min, 1% B; 29.3 min, 55% B; 31.05 min,
214 1% B; 55 min, 1% B; the flow rate was 10 $\mu\text{L}/\text{min}$. In second dimension Acquity UPC²
215 CSH FP and Acquity UPC² BEH were used at 2.0 mL/min and 2.6 mL/min respectively
216 in isocratic conditions, namely $\text{CO}_2/\text{MeOH}/\text{ACN}$ 95/2.5/2.5 (v/v/v) at 45 °C and 140 bar
217 as BPR. The sampling time was 0.3 min. The loop volume of the interface was 3 μL .

218 The conditions of the RPLCxSFC separation of both synthetic sample and aqueous
219 bio-oil extract are given in Tables 2 and 3 respectively.

220 RPLCxRPLC

221 The conditions of the RPLCxRPLC separation of aqueous bio-oil extract are given in
222 Table 3.

223 3 Calculations

224

225 The experimental sample peak capacities were calculated according to

$$226 \quad j_n = \frac{t_n - t_1}{w} \quad (1)$$

227 t_n and t_1 are the retention times of the most and the least retained compound
228 respectively and w is the average 4σ peak width (13.4% of peak height). Exponent j
229 stands for the dimension number.

230

231 Effective sample peak capacities were calculated by the following relationship [10]:

$$232 \quad n_{2D, effective} = \alpha \cdot n \cdot (1 - \gamma) + \gamma \cdot (\alpha \cdot n \cdot n) \quad (2)$$

233 γ is the correction factor corresponding to the ratio of the practical to the theoretical
234 retention area. Its calculation is detailed in reference [6]. α is the undersampling rate
235 introduced by Davis et al. [17] :

$$236 \quad \alpha = \frac{1}{\sqrt{1 + 0.21 \left(\frac{6}{\tau}\right)^2}} \quad (3)$$

237 where τ is the sampling rate of the 2D-separation (i.e. the number of fractions sent to
238 2D per 6σ peak width in 1D).

239

240 2D-data were processed using calculation tools developed under Excel 2007 and
241 Matlab V7.12.0635.

242

243 4 Results and discussion

244 4.1 Theoretical considerations

245

246 The peak capacity in the second dimension n^2 increases with the ratio of the gradient
247 time to the column dead time, t_G/t_0 . It is important to note that the increase in n^2 can
248 be significant in the range of low t_G/t_0 values which are usually considered in the

249 second dimension. It is therefore of prime importance to do everything possible to
250 enhance this ratio. As previously discussed [4], this ratio can be expressed by

251

$$252 \quad \frac{{}^2t_G}{{}^2t_0} = \frac{t_s}{{}^2t_0} - \left[\frac{{}^2V_D}{{}^2V_0} + (1+x) \right] \quad (4)$$

253 where t_s is the sampling time, 2V_D is the 2D dwell volume, 2V_0 is the 2D column dead
254 volume and x is the number of column volume required for 2D column equilibration
255 between two gradient runs.

256 Eq. (4) highlights the need for (i) low 2t_0 and therefore the use of a short 2D column
257 providing high efficiency i.e. packed with sub $2\mu\text{m}$ particles and/or the use of a high
258 linear velocity as that usually required under SFC conditions, (ii) low ${}^2V_D/{}^2V_0$ which is
259 not favorable for SFC as second dimension because a rather large dwell volume is
260 present in the current SFC instrumentation, (iii) few column volumes to equilibrate the
261 2D column (i.e. low x value) and (iv) a substantial sampling time t_s . However t_s affects
262 the injection volume in 2D , 2V_i , according to

$$263 \quad {}^2V_i = t_s \times {}^1F \quad (5)$$

264 Where 1F is the flow-rate in 1D .

265 Critical injection effects have been reported under SFC conditions, especially when
266 using polar injection solvents and/or large injection volumes [18,19]. With RPLC as first
267 dimension, the injection solvent in 2D is composed of water and an organic solvent,
268 typically ACN. To the best of our knowledge, no study has been devoted to hydro-
269 organic mixtures as injection solvents in SFC. Thus, the two following sections present
270 a thorough study to determine the maximum injection volume depending on both
271 mobile phase composition in 1D and stationary phase in 2D .

272 In order to minimize 2V_i and since flow-splitting is impossible between the first RPLC
273 dimension and the second SFC dimension to avoid CO_2 depressurization when the
274 valve is switched, 1F was set at the lowest value ($10 \mu\text{L}/\text{min}$) recommended in gradient
275 elution for the UHPLC instrument. As a result a 1mm i.d. column was found to be the
276 most appropriate column geometry for the first dimension.

277

278 *4.2 Effect of injection of a large water volume on inlet pressure increase*

279

280 In SFC, when the injection solvent contains water, we observed a pressure increase
281 (denoted ΔP) which occurs a few seconds after the injection process. Then, the
282 pressure slowly decreases to its initial value. This phenomenon is shown in Fig.3a for
283 1D-SFC conditions and in Fig.3b for a ²D run in RPLC x SFC conditions. The injection
284 process is different between these two configurations. In 1D-SFC, the sample is
285 pressurized before injection thanks to a particular design of the UPC² injection system.
286 This pressurization step results in an immediate sharp pressure increase followed by
287 a sharp decrease down to the working pressure. In RPLC x SFC the injection system
288 of the UPC² instrument is not used. The sample is sent from the ¹D RPLC column to
289 the sample loop and then injected in the SFC ²D column when the 10-port valve is
290 switched. As a result, the preceding sharp increase does not occur. However, in both
291 cases, the same pressure increase ΔP can be observed. We have measured ΔP under
292 different conditions in 1D-SFC. The experiments were focused on the behavior of 4
293 different SFC stationary phases subjected to 3 different injection volumes (1, 5 and 10
294 μL) with 3 different injection solvents differing in their water content (95%, 50% and
295 5%). Among the four studied stationary phases, two were fairly apolar (Acquity CSH
296 FP and Acquity HSS C18) while two were significantly polar (Acquity BEH and Acquity
297 BEH-2EP). The obtained results, given in Fig.4, clearly show that ΔP increases both
298 with the injection volume and with the percentage of water in the injection solvent. It is
299 also very interesting to note that the pressure increase is markedly higher with less
300 polar stationary phases (Figs. 4a and 4b) resulting in an inlet pressure exceeding the
301 pressure limit authorized by the instrument for 10 μL injected in 95 % water. In this
302 situation, ΔP was much higher than 80bar while it remained lower than 40bar for the
303 two polar stationary phases (Figs. 4c and 4d). For 5 μL injected, ΔP is still high on less
304 polar stationary phases compared to polar stationary phases (50 vs 5 bar at 95 % water
305 and 10 vs 2 bar at 50%water).

306 The problem of pressure increase was found to be much more critical during a RPLC
307 x SFC separation as highlighted in Fig.5. The inlet pressure of the ²D SFC instrument
308 was recorded when an Acquity CSH FP column (Fig.5a) and an Acquity BEH column
309 were used in ²D (Fig.5b). SFC conditions were strictly identical for both columns,
310 except flow rate set at 2.0 mL/min and 2.6 mL/min for Acquity CSH FP and Acquity
311 BEH respectively. The sampling time was 0.3 min. Consequently 3 μL of liquid solvent
312 were injected in the ²D SFC column every 0.3 min. The composition of this liquid

313 injection solvent changes gradually as the gradient in the ¹D column progresses. This
314 variation is easily assessed by means of the ¹D gradient profiles given in Figs. 5a and
315 5b. With an apolar stationary phase (Fig.5a), whereas the inlet pressure at the time of
316 injection was 315 bar, it reached 400 bar after 10 runs. This pressure that is very close
317 to the instrument pressure limit was kept nearly constant during 20 minutes before
318 slowly decreasing down to the initial inlet pressure when the percentage of water
319 becomes lower than 70%. This phenomenon was not observed with polar stationary
320 phases (Fig.5b). To explain this, we suggest that, unlike polar stationary phases, apolar
321 ones are poorly wetted by injection solvents rich in water, which finally results in local
322 change of mobile phase nature. Due to the short analysis time in the second SFC
323 dimension (0.3 min), these successive modifications have no time to be swept away.
324 They eventually accumulate to form a multiphase plug (composed of CO₂, water,
325 MeOH and ACN) which is more viscous than the original monophasic mobile phase
326 (CO₂-MeOH-ACN mixture).

327 In addition to this critical problem of pressure increase with apolar stationary phases
328 which prevents from working in at high flow-rates in ²D, significant baseline fluctuations
329 are observed for the fractions that are separated during the pressure plate (Fig.2c).
330 Conversely no baseline fluctuation is noted for fractions that are analyzed when the
331 inlet pressure is back to normal (Fig.5e). With ²D polar stationary phases the ²D inlet
332 pressure remains constant during the whole RPLC x SFC separation (Fig.5b) and no
333 disruption of the baseline is visible whatever the considered fractions (Figs. 5d and 5f).

334 In the light of these results, it is clear that a polar stationary phase should be preferably
335 used for the SFC second dimension. Re-injection of very low injection volumes (<1 μL)
336 in ²D could probably circumvent the problems encountered with apolar stationary
337 phase but it should lead to quite unrealistic sampling time (< 0.1min). Another
338 alternative would be to start the RPLC gradient with a water content lower than 70%.
339 However this option is not possible for compounds that are poorly retained in RPLC
340 such as small polar compounds. Considering the above results, Acquity BEH-2EP was
341 chosen as ²D SFC stationary phase for the rest of this study.

342 4.3 *Effect of injection volumes and injection solvent composition on peak shapes in* 343 *1D-SFC*

344

345 in SFC, it was recently shown [19] that the injection solvent composition strongly
346 influences peak shapes. Very polar solvents such as DMSO and MeOH were found to
347 lead to significant peak distortions even for low injected volumes, these distortions
348 being more pronounced for less retained compounds. Abrahamsson et al. [18] also
349 studied the effect of various injection solvents in accordance with the stationary phase.
350 They pointed out that injection solvent may interact with stationary phase, mobile
351 phase and solute, thereby affecting either positively or negatively peak shape.
352 However the effect of water as injection solvent on peak shape has never been studied
353 neither as pure solvent, probably due to the fact that it is highly polar and not much
354 miscible with CO₂, nor combined with other solvents. Here, we have studied the impact
355 of injected volume on peak shape when the solute is dissolved in different water/ACN
356 mixtures. Results obtained with CO₂/ACN/MEOH 95/2.5/2.5 (v/v/v) as SFC mobile
357 phase and o-cresol as solute are shown in Fig.6. Surprisingly, when the injected
358 volume does not exceed 5 μL (i.e. 5% of the column dead volume), a very high content
359 of ACN in injection solvent seems to be more damaging for the peak shape than a high
360 content of water (Figs.6a and 6b). It is possible to inject up to 5 μL of sample dissolved
361 in a solvent containing 50 to 95% water without strong peak distortion. Obviously, for
362 10 μL injected (Fig.6c) which represents 10% of the column dead volume, the peak
363 shapes are very bad for all studied injection solvents. The results shown in Fig.6 also
364 point out the retention shift that increases with both the percentage of water in the
365 injection solvent and the injection volume. It is likely to be due to two combined effects:
366 (i) good affinity of water for the polar sites of the stationary phase and (ii) high affinity
367 of o-cresol for water. Consequently, when the injection plug enters the column, o-cresol
368 interacts preferentially with the stationary phase thereby increasing retention. Such
369 retention shift could be damaging for 2D-chromatogram reconstruction due to difficulty
370 in peak assignment between consecutive fractions analysis. However, this problem
371 does not really arise in RPLC x SFC since the injection solvent composition slightly
372 varies between the 2 to 4 consecutive ²D runs that are required in comprehensive two-
373 dimensional chromatography to minimize undersampling [17].

374 In view of this study, it was decided to inject a maximum of 5μL in the second SFC
375 dimension. Since flow splitting between ¹D and ²D was not possible with a LCxSFC
376 configuration, injection volume in ²D was directly related to both ¹D flow-rate and
377 sampling time. Accordingly, with 10μL/min as ¹D flow-rate, the sampling time could not
378 be higher than 30s.

380 4.4 Application to the RPLC x SFC separation of a sample of aromatic compounds

381
382 In order to validate the choices made previously to carry out the on-line RPLCxSFC
383 experiments, 12 aromatic compounds were separated. The experimental conditions
384 are given in Table 2. The sampling time and the ¹D flow rate being equal to 0.5 min
385 and 10 μ L/min respectively, two identical sample loops of 5 μ L were installed on the
386 10-port switching valve in order to completely fill the sample loop. This configuration
387 avoids dissolving issues as highlighted in Fig.7. When the sample loop is in inject
388 position, it is filled with the SFC mobile phase. When the sample loop comes back in
389 load position it is depressurized, allowing some droplets of organic modifier covering
390 the walls of the loop. Whereas this droplets can be well solubilized in the RPLC mobile
391 phase coming from ¹D (Fig.7a) they may cause troublesome issues with the SFC
392 mobile phase if the sample loop is partially filled (Fig.7b). In addition the presence of
393 air to push the sample plug can be detrimental compared to the SFC mobile phase
394 which is better dissolved in the hydro-organic liquid solvent. The obtained RPLCxSFC
395 separation is presented in Fig.8a. It is interesting to notice the large occupation of the
396 retention space by the 12 compounds, underlining the great interest of this coupling in
397 terms of orthogonality. Furthermore, as highlighted in Fig.8b showing the separation of
398 four consecutive fractions, peak shapes are quite symmetrical as could be expected
399 from our preliminary studies. With 0.83s as average 4σ peak width the sample peak
400 capacity is close to 15 in the second dimension.

401

402 4.5 Comparison of RPLC x RPLC and RPLC x SFC systems for the separation of a 403 bio-oil sample

404

405 An RPLCxSFC experiment was carried out on a real sample consisting in an aqueous
406 extract of a bio-oil. The conditions of the first dimension were similar to those used in
407 a previous study [10] except the gradient time that is much lower in the present work.
408 In order to elute all the compounds in ²D SFC conditions, a gradient from 15% to 50 %
409 MeOH/ACN (1:1) is needed. The contour plot of the RPLCxSFC separation is
410 presented in Fig.9a. For comparison, Fig.9b shows the RPLCxRPLC separation of the
411 same sample performed using the same ¹D conditions as the RPLCxSFC separation.

412 For a better comparison of the two separations, the sampling time was also kept
413 identical (i.e. 30s). As a consequence, 1n and α were identical for both separations.
414 Experimental conditions are given in Table 3.

415 Fig. 9 clearly underlines that the RPLCxSFC system offers much higher degree of
416 orthogonality (γ close to 1) compared to the RPLCxRPLC configuration (γ close to 0.6).
417 It is important to note that this latter configuration and the corresponding conditions
418 displayed in Table 3 were found to provide the highest effective peak capacity among
419 the different studied RPLCxRPLC systems [10]. In RPLCxSFC, the enhancement of
420 the available separation space allows to reach an effective peak capacity slightly
421 higher in spite of a higher 2n with RPLCxRPLC conditions (see Table 4). Several
422 reasons could explain why 2n is higher with RPLC as second dimension:

423 (i) $^2t_G/2t_0$ ratio was more than three times higher for RPLCxRPLC (5.4 vs 1.7 for
424 RPLCxSFC) leading to a higher peak capacity in second dimension according to eq.
425 (4) and as discussed in section 4.1. Indeed, despite a $^2t_s/2t_0$ ratio in favor of RPLCxSFC
426 due to the higher flow rate used in SFC (2.0 mL/min vs 1.2 mL/min in RPLC), the dwell
427 volume is larger in SFC (300 μ L vs 120 μ L in LC) increasing $^2V_D/2V_0$ ratio. Moreover,
428 for software reasons, an extra-time of 0.2 min had to be added between two
429 consecutive runs of second dimension in SFC, thereby leading to a real acquisition
430 time of only 0.3 min. As a consequence, while the number of column volumes used for
431 column equilibration, x , was set at 2 for RPLC as second dimension, x was equal to 4
432 for SFC, which therefore significantly decreased $^2t_G/2t_0$ ratio. It was shown that only two
433 column dead volumes ($x=2$) can provide a good run-to-run repeatability in UHPLC
434 conditions [20–22] which was also found to be suitable for SFC conditions for neutral
435 compounds (data not shown).

436 (ii) The extra-column variance is markedly higher with SFC apparatus compared to
437 UHPLC apparatus and led to an important loss of efficiency especially for 50x2.1 mm
438 column [23]. In our case the extra-column variance in 2D was 3.5 times larger in
439 RPLCxSFC (32 μ L² vs 9 μ L² in RPLCxRPLC). This is mainly due to both larger tubing
440 i.d. and larger flow-cell volume of the UV detector used in SFC (175 μ m and 16 μ L
441 respectively) compared to those used in RPLC (65 μ m and 0.5 μ L respectively).

442 (iii) Some significant injection effects still exist in RPLCxSFC whereas none were
443 observed in RPLCxRPLC. The compatibility of the mobile phases of the two
444 dimensions is more challenging in RPLCxSFC which may involve more critical injection
445 effects. Moreover, while all the peaks in the ²D RPLC have nearly the same width (i.e.

446 0.6s), the peak shapes obtained in ²D SFC were not similar with $w_{4\sigma}$ varying from 0.51
447 s to 1.50 s depending on the compounds. As a result the average measured peak width
448 at 4σ was 0.60 s in RPLC compared to 1.09 s in SFC conditions. More pronounced
449 injection effects, resulting in a loss of column efficiency, could also probably explain
450 the 7-fold loss in sensitivity when using SFC as second dimension compared to RPLC
451 making RPLCxSFC less attractive in terms of sensitivity.
452 Finally, despite the raised instrumental issues, the present results show that
453 RPLCxSFC can be a good alternative to RPLCxRPLC for the separation of biomass
454 by-products
455

456 **5 Conclusions**

457

458 The goal of this work was to evaluate the potential of on-line RPLCxSFC for the
459 separation of aromatic compounds. Suitable stationary phase and injection volume for
460 the ²D SFC were chosen thanks to preliminary studies aiming at overpassing the lack
461 of compatibility between the mobile phases used as first and second dimension. Polar
462 stationary phases in SFC seem to be the most adapted stationary phases. On the other
463 hand it was shown that a maximum of 5 μ L of a mixture of water/acetonitrile was
464 appropriate to inject in the second SFC dimension. An on-line RPLCxSFC separation
465 of a real aqueous bio-oil sample was successfully carried out achieving full
466 orthogonality ($\gamma=1$), while with an optimized RPLCxRPLC separation γ could not
467 exceed 0.59. Accordingly, although wider peaks were observed in SFC as second
468 dimension, the effective peak capacity was slightly higher with RPLCxSFC
469 configuration (620 vs 560 with RPLCxRPLC). However, it should be noted that the
470 peak capacity in ²D SFC was limited by the high dwell volume of the apparatus as well
471 as software issues due to this unusual coupling. Consequently, we are sure that there
472 is still room for further improvements. Yet, sensitivity was found markedly higher with
473 the RPLCxRPLC separation due to an important extra-column variance with the SFC
474 system and still pronounced injection effects in SFC. Finally, in the light of these
475 results, on-line RPLCxSFC can be considered as an interesting alternative for the
476 separation of neutral compounds compared to RPLCxRPLC.
477

478 **Acknowledgements**

479

480 M.S., S.H. and G.C. wish to thank Waters for the loan of the UPC² system and
481 especially Philippe Mériquier for his help in LCxSFC setting up. S.H. would like to thank
482 Davy Guillaume for stimulating discussions and valuable advice on different aspects of
483 SFC.

484

485

- 486 [1] P. Dugo, F. Cacciola, T. Kumm, G. Dugo, L. Mondello, *J. Chromatogr. A* 1184
487 (2008) 353.
- 488 [2] I. François, K. Sandra, P. Sandra, *Anal. Chim. Acta* 641 (2009) 14.
- 489 [3] P.Q. Tranchida, P. Donato, F. Cacciola, M. Beccaria, P. Dugo, L. Mondello, *TrAC*
490 *Trends Anal. Chem.* 52 (2013) 186.
- 491 [4] M. Sarrut, G. Crétier, S. Heinisch, *TrAC Trends Anal. Chem.* 63 (2014) 104.
- 492 [5] G. Guiochon, N. Marchetti, K. Mriziq, R.A. Shalliker, *J. Chromatogr. A* 1189
493 (2008) 109.
- 494 [6] A. D'Attoma, C. Grivel, S. Heinisch, *J. Chromatogr. A* 1262 (2012) 148.
- 495 [7] I. François, A. De Villiers, P. Sandra, *J. Sep. Sci.* 29 (2006) 492.
- 496 [8] K.J. Mayfield, R.A. Shalliker, H.J. Catchpole, A.P. Sweeney, V. Wong, G.
497 Guiochon, *J. Chromatogr. A* 1080 (2005) 124.
- 498 [9] P. Jandera, *J. Sep. Sci.* 29 (2006) 1763.
- 499 [10] A. Le Masle, D. Angot, C. Gouin, A. D'Attoma, J. Ponthus, A. Quignard, S.
500 Heinisch, *J. Chromatogr. A* 1340 (2014) 90.
- 501 [11] D. Tomasini, F. Cacciola, F. Rigano, D. Sciarrone, P. Donato, M. Beccaria, E.B.
502 Caramão, P. Dugo, L. Mondello, *Anal. Chem.* 86 (2014) 11255.
- 503 [12] G. Guiochon, A. Tarafder, *J. Chromatogr. A* 1218 (2011) 1037.
- 504 [13] C. West, E. Lesellier, *J. Chromatogr. A* 1110 (2006) 191.
- 505 [14] A. Grand-Guillaume Perrenoud, J.-L. Veuthey, D. Guillaume, *J. Chromatogr. A*
506 1266 (2012) 158.
- 507 [15] I. François, P. Sandra, *J. Chromatogr. A* 1216 (2009) 4005.
- 508 [16] P.G. Stevenson, A. Tarafder, G. Guiochon, *J. Chromatogr. A* 1220 (2012) 175.
- 509 [17] J.M. Davis, D.R. Stoll, P.W. Carr, *Anal. Chem.* 80 (2008) 461.
- 510 [18] V. Abrahamsson, M. Sandahl, *J. Chromatogr. A* 1306 (2013) 80.
- 511 [19] J.N. Fairchild, J.F. Hill, P. Iraneta, *LC-GC N. Am.* 31 (2013) 326.
- 512 [20] A.P. Schellinger, D.R. Stoll, P.W. Carr, *J. Chromatogr. A* 1192 (2008) 41.
- 513 [21] A.P. Schellinger, D.R. Stoll, P.W. Carr, *J. Chromatogr. A* 1192 (2008) 54.
- 514 [22] C. Grivel, J.-L. Rocca, D. Guillaume, J.-L. Veuthey, S. Heinisch, *J. Chromatogr.*
515 *A* 1217 (2010) 459.
- 516 [23] A. Grand-Guillaume Perrenoud, C. Hamman, M. Goel, J.-L. Veuthey, D.
517 Guillaume, S. Fekete, *J. Chromatogr. A* 1314 (2013) 288.

518

519 Figure captions :

520 Figure 1 : RPLCxSFC setup. (a) The eluent of first dimension is stored in loop 1 while
521 the content of loop 2 is injected in second dimension and (b) vice versa

522 Figure 2 : Influence of gradient profile on the dwell volume measurement in SFC.
523 Mobile phases : A=CO₂, B=MeOH+0.1% acetone. Temperature = 30 °C. BPR = 140
524 bar. Detection Wavelength = 254 nm. Programmed gradient : (a) 1-99 %B in 8 min at
525 1 mL/min, (b) 69-99 %B in 3 min at 1.5 mL/min. Dotted lines are the tangents to the
526 obtained gradient profile. Δt represents the uncertainty at half part of the UV signal with
527 t^* being the corresponding time.

528 Figure 3 : Observed inlet pressure of the SFC instrument vs run time in (a) 1D-SFC
529 and (b) RPLC x SFC. Conditions common to all experiments : injection solvent =
530 Water/ACN 95/5 (v/v) ; mobile phase = CO₂/MeOH/ACN 95/2.5/2.5 (v/v/v) ; column =
531 Acquity UPC² CSH FP 50x2.1 mm, 1.7 μ m ; temperature = 45°C ; BPR = 140 bar.
532 Other conditions : (a) flow rate = 2.7 mL/min, injected volume = 5 μ L ; (b) flow rate =
533 2.0 mL/min, injected volume = 3 μ L. ΔP represents the pressure increase (see text for
534 more details)

535 Figure 4 : Pressure increase ΔP in 1D-SFC as a function of water content of the
536 injection solvent and injection volume V_i on (a) Acquity UPC² CSH FP column, (b),
537 Acquity UPC² HSS C18 column, (c) Acquity UPC² BEH column and (d) Acquity UPC²
538 BEH-2EP column. Column geometry : 50x2.1 mm, 1.7 μ m ; flow rate = 2.7 mL/min ;
539 temperature = 45°C ; BPR = 140 bar ; injection solvent = mixture of water and
540 acetonitrile. * means that ΔP could not be measured because the pressure limit (414
541 bar) was reached.

542 Figure 5: Influence of ²D stationary phase on the course of a RPLCxSFC experiment.
543 (a) and (b) : SFC inlet pressure versus run time. c) and (d) : ²D analysis of fractions
544 eluted from ¹D between 20.1 and 21.0 min. (e) and (f) : ²D analysis of fractions eluted
545 from ¹D between 36.3 and 37.2 min. Sampling time = 0.3 min. RPLC conditions :
546 column dimensions = 50x1.0 mm, stationary phase = 3.5 μ m Xbridge C18, solvent A
547 = water, solvent B = ACN, gradient from 1% B to 55 % B in 29.3 min, flow rate = 10
548 μ L/min, temperature = 30 °C. SFC conditions : column dimensions = 50x2.1 mm,
549 stationary phase = (a,c,e) 1.7 μ m Acquity UPC² CSH FP ; (b,d,f) 1.7 μ m Acquity UPC²
550 BEH, isocratic mobile phase = CO₂/MeOH/ACN 95/2.5/2.5 (v/v/v), flow rate = (a,c,e)
551 2.0 mL/min ; (b,d,e) 2.6 mL/min, temperature = 45 °C, BPR = 140 bar. Full lines shows

552 the gradient profile in ¹D outlet. Dotted lines show the time windows for the selected
553 fractions.

554 Figure 6 : Effect of injection solvent and injected volume peak shape. Solute : o-cresol
555 with (a) 1 μ L, (b) 5 μ L, (c) 10 μ L. Injection solvent composition: Water/ACN 95/5 (v/v)
556 (—), 50/50 (v/v) (—) and 5/95 (v/v) (—). Column : Acquity UPC² BEH-2EP, 50x2.1
557 mm, 1.7 μ m. Flow rate = 2.2 mL/min; mobile phase: CO₂/MeOH/ACN 95/2.5/2.5 (v/v/v).
558 Temperature = 45°C. BPR = 140 bar. Detection wavelength = 215 nm (compensation
559 from 350 nm to 450 nm).

560 Figure 7 : schematic representation of injection process in the second dimension of
561 RPLCxSFC with (a) completely and (b) partially filling of the loops

562 Figure 8 : On-line RPLCxSFC separation of 12 aromatic compounds. (a) contour plot
563 UV and (b) overlay of SFC separation of the fractions from 27 min to 28.5 min (red
564 dotted lines in the contour plot). See Table 1 for solutes and Table 3 for experimental
565 conditions.

566 Figure 9 : Comparison (a) on-line RPLCxSFC and (b) on-line RPLCxRPLC separation
567 of a bio-oil aqueous extract. Experimental conditions are summarized in Table 3. The
568 red dotted lines in (b) delimit the separation space.

569

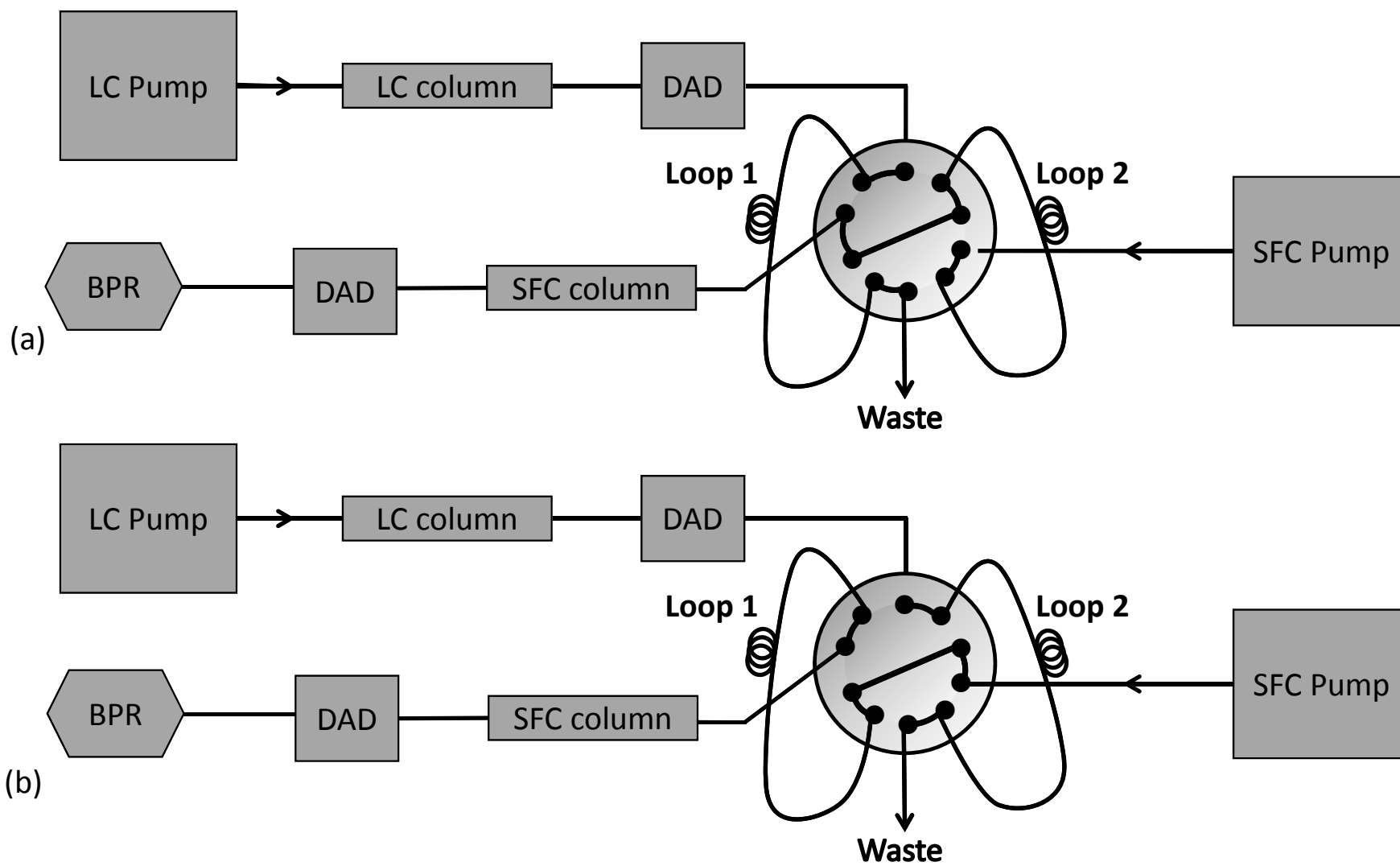


Figure 1 :

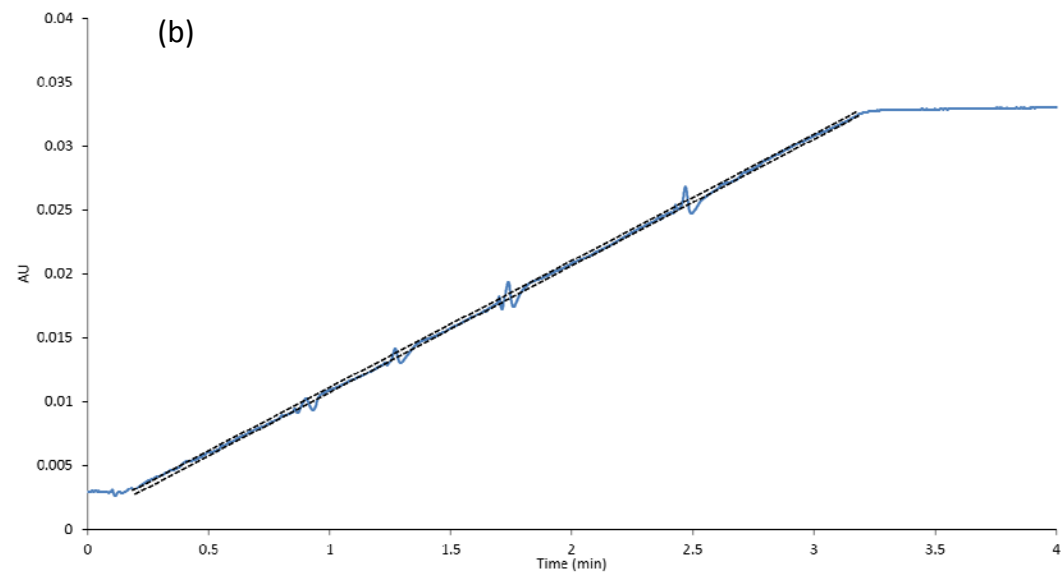
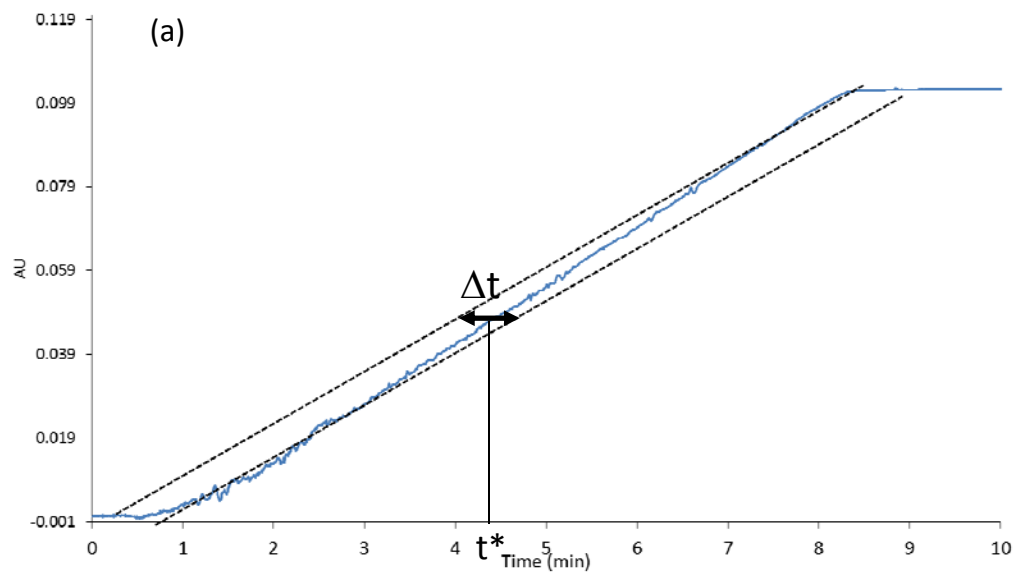


Figure 2

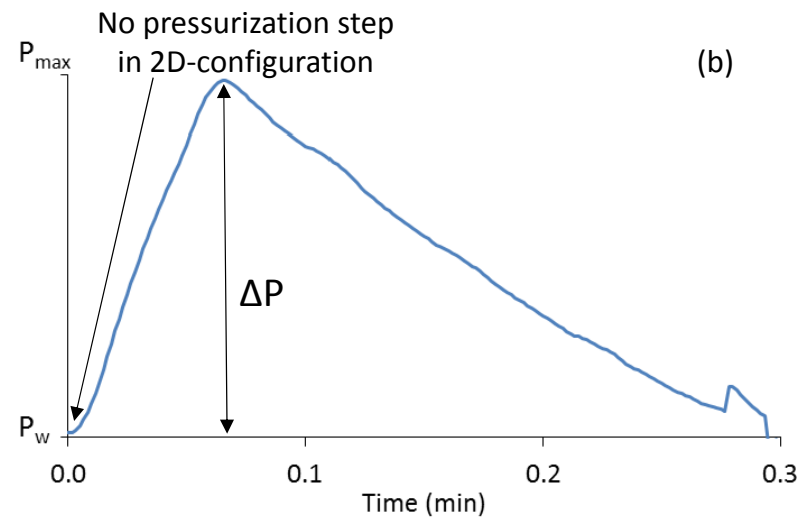
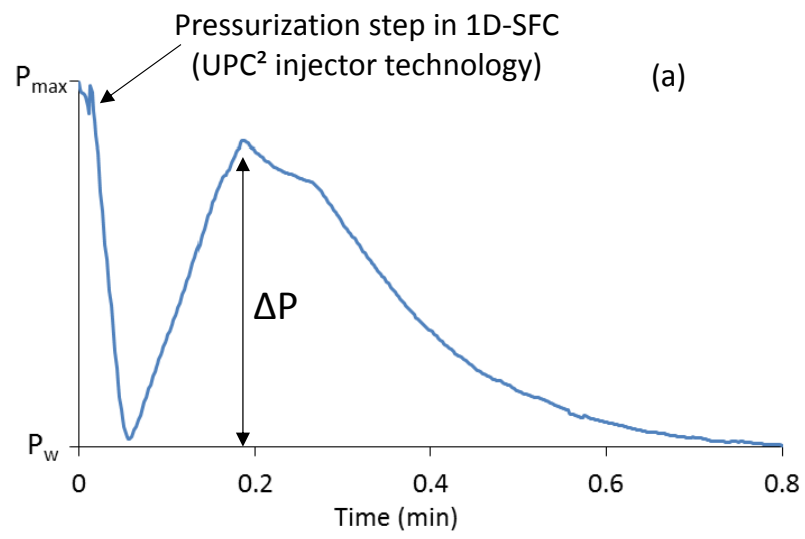


Figure 3

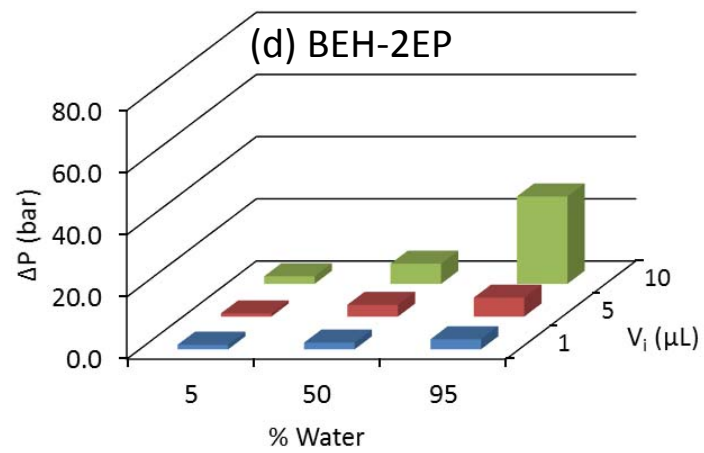
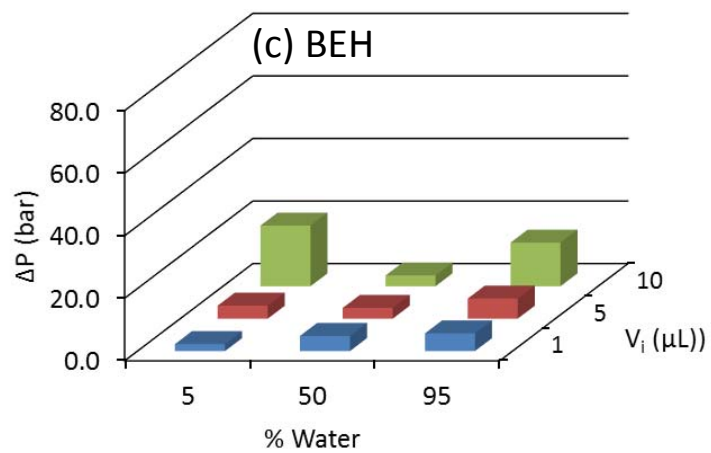
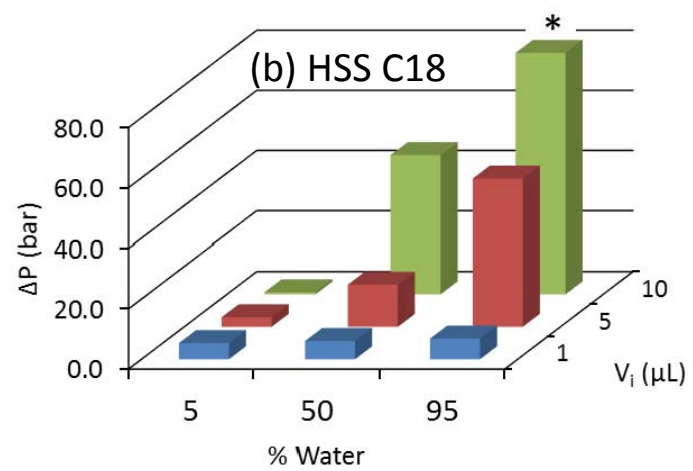
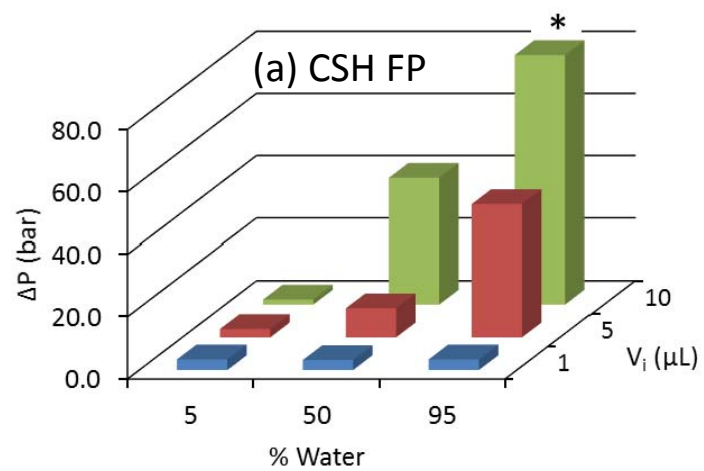


Figure 4

CSH FP column

BEH column

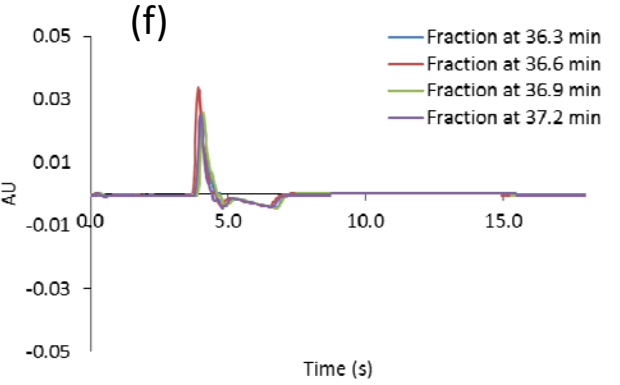
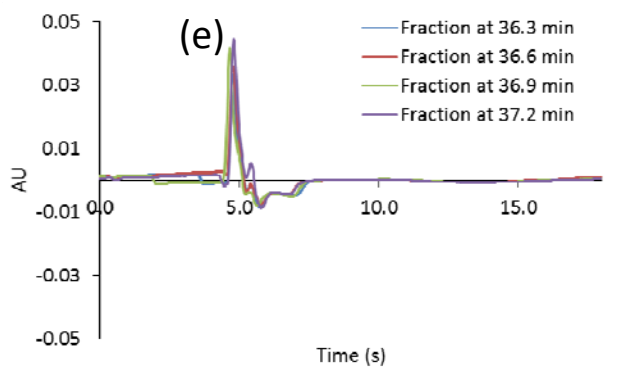
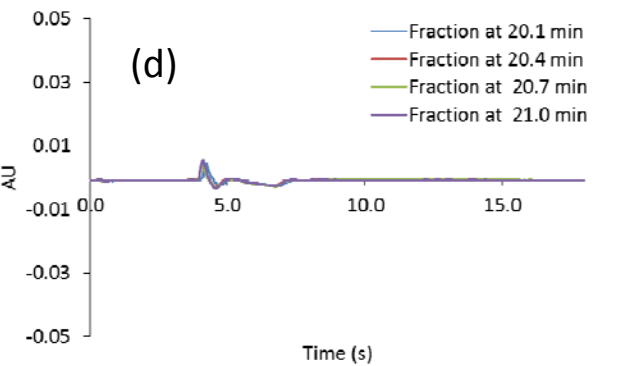
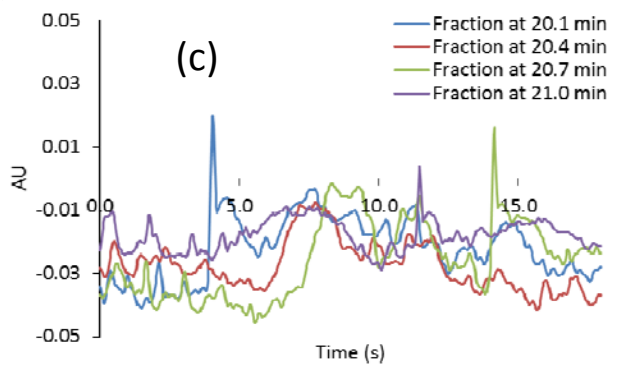
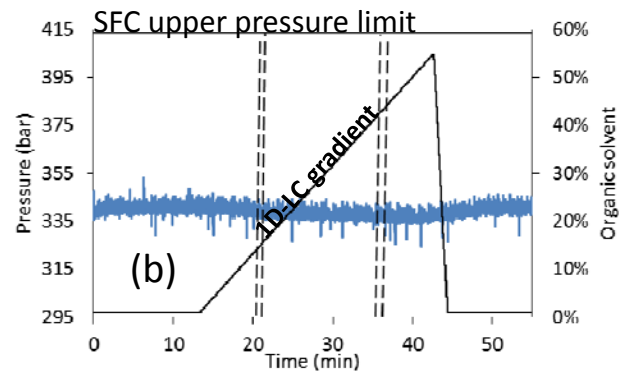
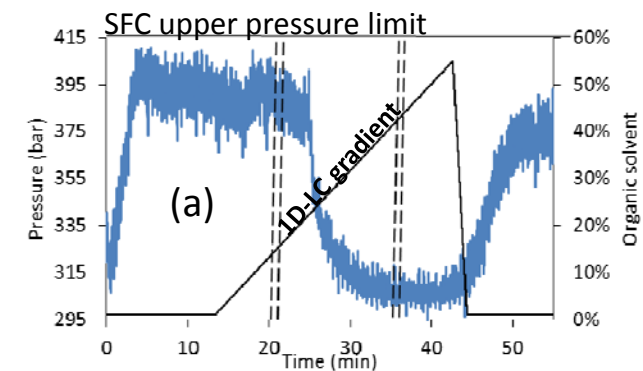


Figure 5

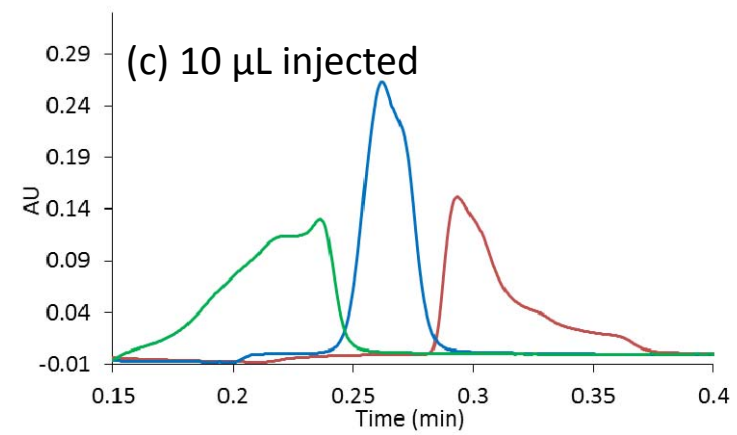
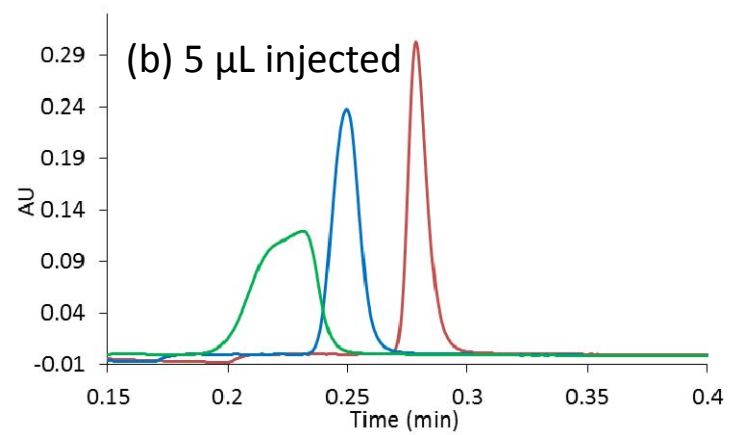
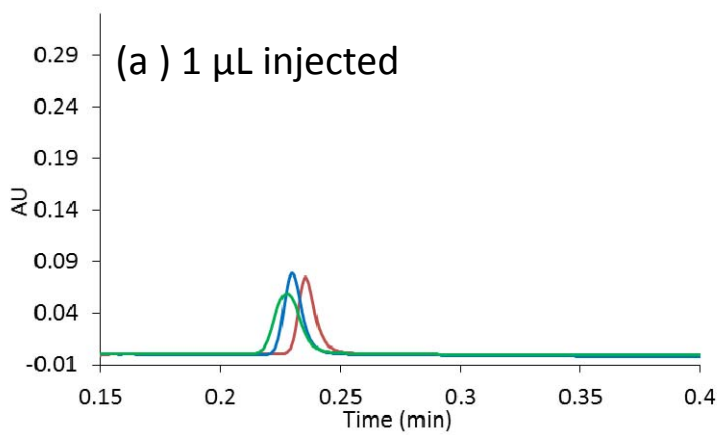


Figure 6

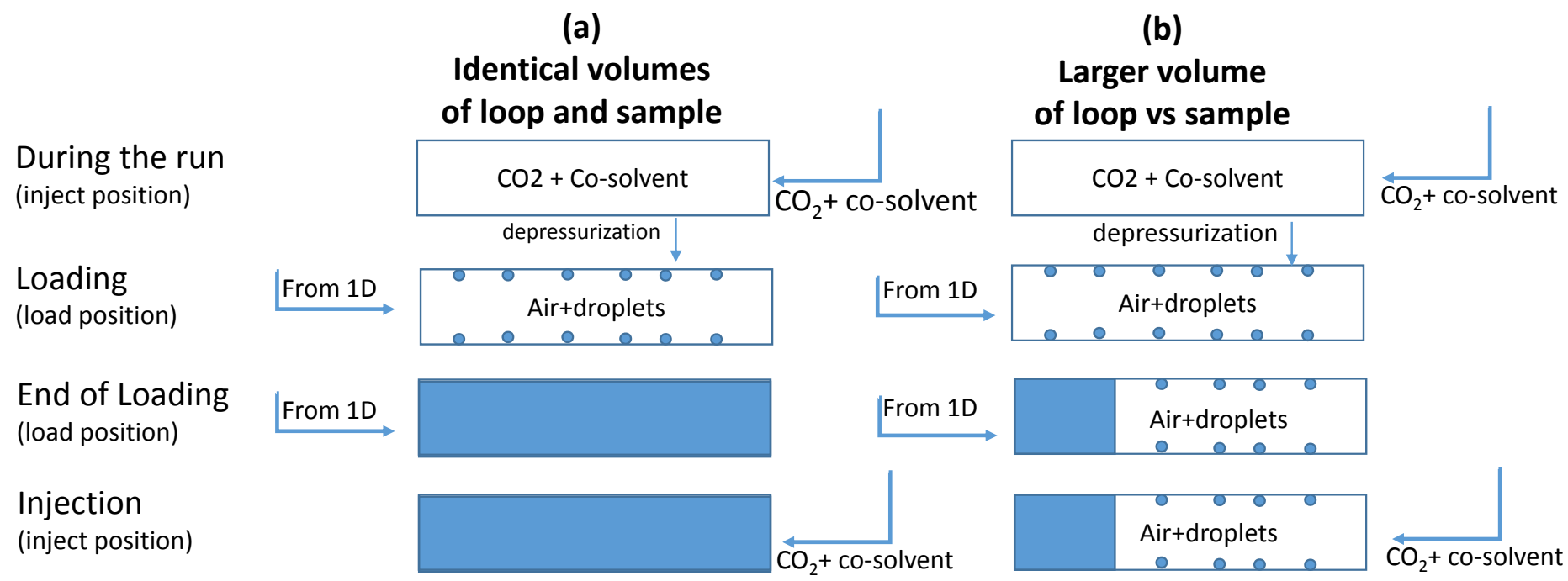


Figure 7

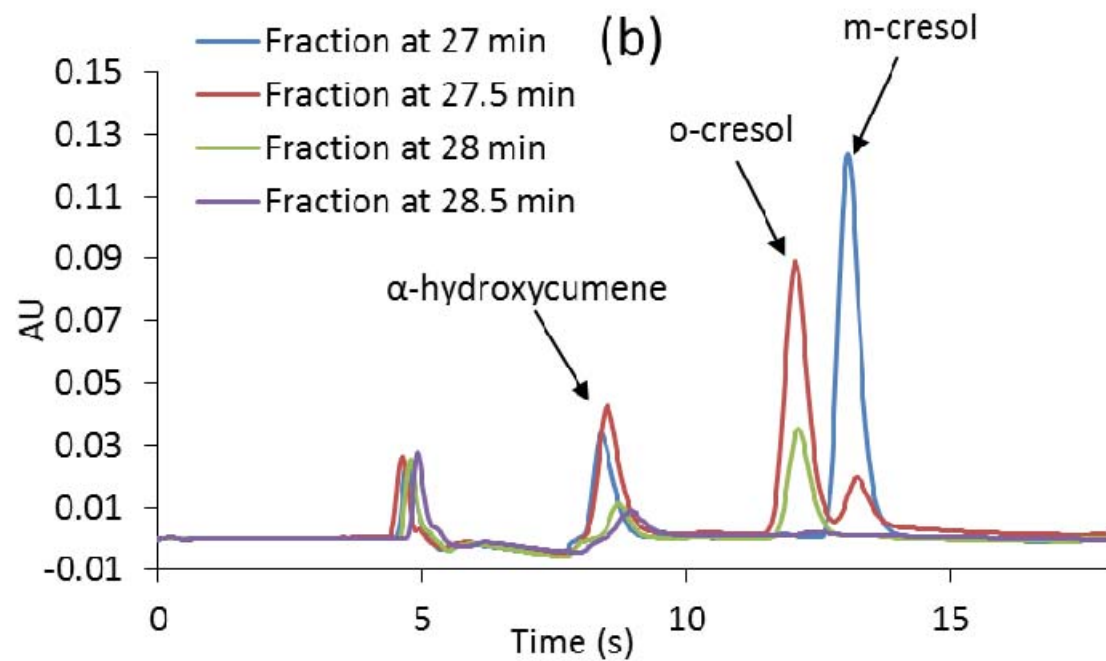
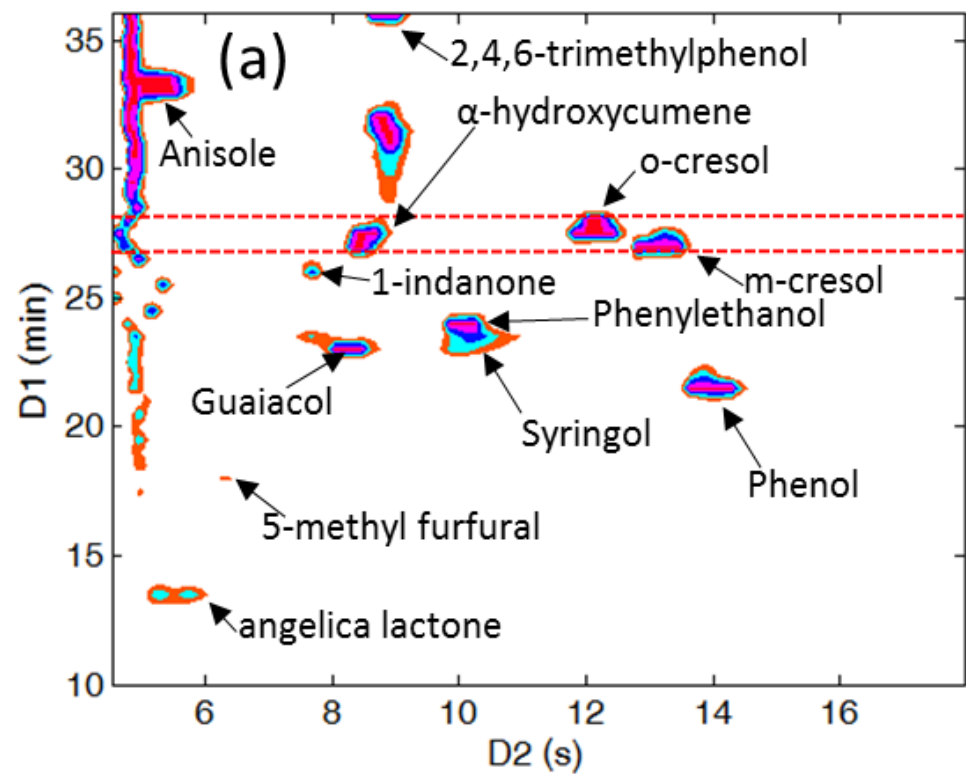
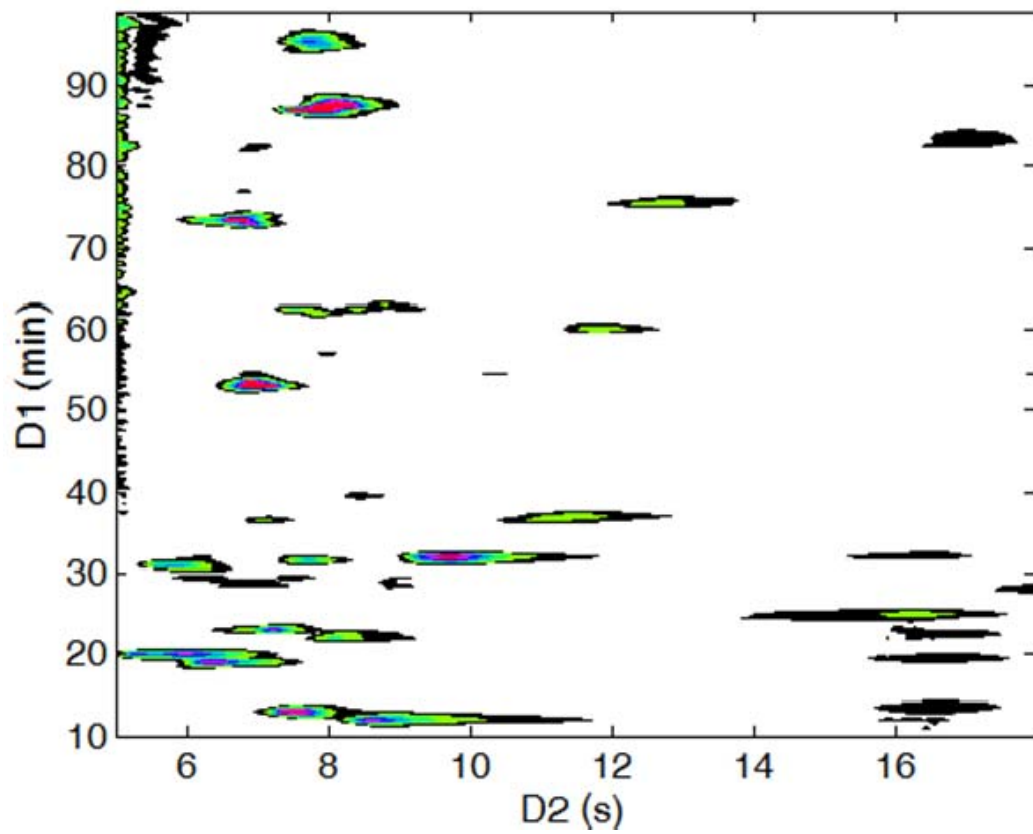


Figure 8

(a) RPLCxSFC



(b) RPLCxRPLC

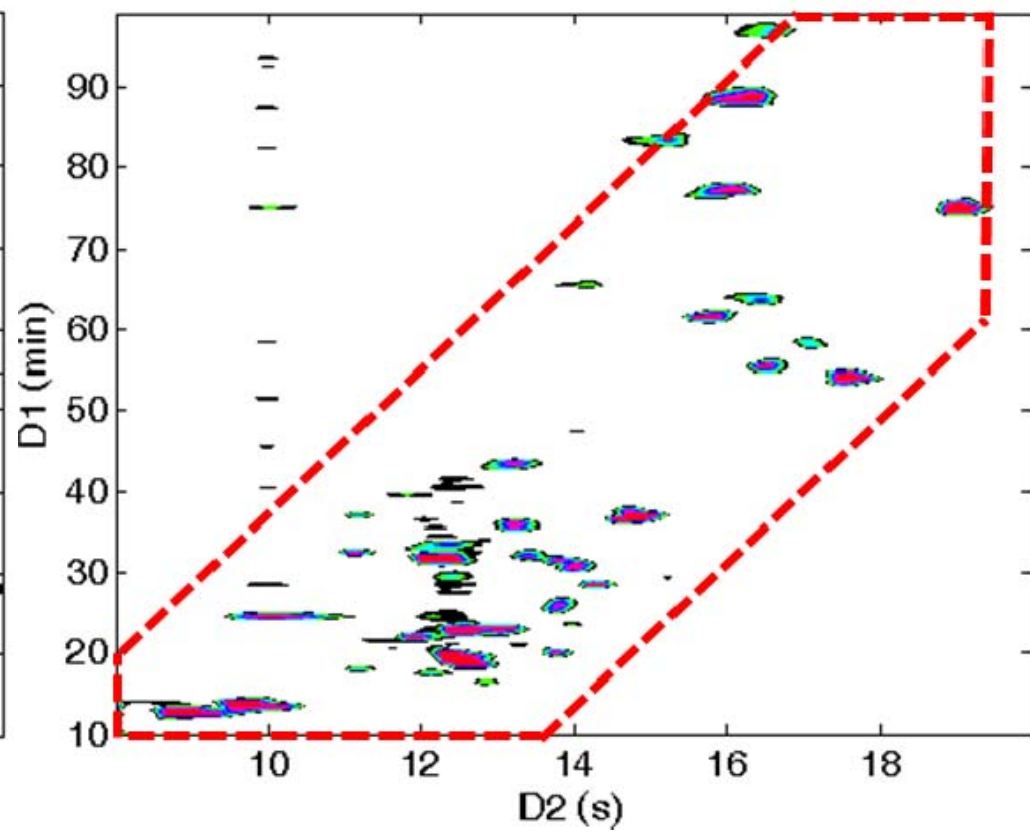


Figure 9

1 Table 1 - Physical and chemical properties of some bio-oil representative compounds

	Compound	Chemical family	Molecular Formula	MW (g/mol)	log P
1	α -angelica lactone	lactone	C ₅ H ₆ O ₂	98.10	0.236
2	2-phenylethanol	alcohol	C ₈ H ₁₀ O	122.16	1.504
3	5-methylfurfural	furan	C ₆ H ₆ O ₂	110.11	0.670
4	phenol	phenol	C ₆ H ₆ O	94.11	1.540
5	o-cresol	phenol	C ₇ H ₈ O	108.14	1.962
6	m-cresol	phenol	C ₇ H ₈ O	108.14	2.043
7	2,4,6-trimethylphenol	phenol	C ₉ H ₁₂ O	136.19	2.935
8	α -hydroxycumene	phenol	C ₉ H ₁₂ O	136.19	2.861
9	guaiacol	guaiacol	C ₇ H ₈ O ₂	124.14	1.341
10	syringol	syringol	C ₈ H ₁₀ O ₃	154.16	1.218
11	1-indanone	enone	C ₉ H ₈ O	132.16	1.419
12	anisole	aromatic ether	C ₇ H ₈ O	108.14	2.170

- 1 Table 3 – Experimental conditions for both RPLCxSFC and RPLCxRPLC separations
 2 of the bio-oil aqueous sample

	RPLC (¹ D)	SFC (² D)	RPLC (² D)
Stationary phase	Hypercarb	Acquity UPC ² BEH-2EP	Acquity CSH Phenyl Hexyl
Column geometry	100x1.0 mm, 5 μm	50x2.1 mm, 1.7 μm	50x2.1 mm, 1.7 μm
Mobile phase	A : Water B : ACN	A : CO ₂ B : MeOH/ACN 1:1 (v/v)	A : Water + 0.1 % FA* B : ACN + 0.1 % FA
Flow rate	10 μL/min	2 mL/min	1.2 mL/min
Gradient	5 to 99 % (B) in 102.5 min	15 to 50% (B) in 0.12 min	5 to 55% (B) in 0.18 min
BPR	/	140 bar	/
Temperature	30 °C	45 °C	80 °C
UV	220 nm	220 nm Compensation from 350 to 450 nm	220 nm
Injected volume	5 μL	5 μL	5 μL

3 0.5 min as sampling time

4 * FA means formic acid

- 1 Table 2 – Experimental conditions for the RPLCxSFC separation of the 12
 2 representative compounds (see list in table 1)

	RPLC (¹ D)	SFC (² D)
Stationary phase	X Bridge BEH C18	Acquity UPC ² BEH-2EP
Column geometry	50x1.0 mm, 3.5 μm	50x2.1 mm, 1.7 μm
Mobile phase	A : Water B : ACN	A : CO ₂ B : MeOH/ACN 1:1 (v/v)
Flow rate	10 μL/min	2 mL/min
Gradient	8 to 51 % (B) in 23 min	Isocratic 5% (B)
BPR	/	140 bar
Temperature	30 °C	45 °C
UV	220 nm	215 nm (compensation from 350 to 450 nm)
Vinj	2 μL	5 μl

- 3 0.5 min as sampling time

1 Table 4 – Experimental results of RPLCxSFC and RPLCxRPLC

	γ	α	1n	$^2W_{4\sigma}$ (s)	2n	$^1n \cdot ^2n$	$n_{2D, effective}$
RPLCxSFC	1	0.85	56	1.09	13	730	620
RPLCxRPLC	0.59	0.85	56	0.60	20	1120	560

2

3 1n and 2n were calculated according to eq.1

4 γ was calculated according [6]

5 α was calculated according to eq.3

6 $n_{2D, effective}$ was calculated according to eq.2